Materials Letters 107 (2013) 291–294

Contents lists available at SciVerse ScienceDirect

Materials Letters

journal homepage: www.elsevier.com/locate/matlet

Hydrothermal synthesis of $CuBi_2O_4$ nanosheets and their photocatalytic behavior under visible light irradiation

Yahong Xie [a,b,*], Yun Zhang [a], Guihua Yang [a], Chunhui Liu [a], Jide Wang [a]

[a] Key Laboratory of Oil and Gas Fine Chemicals, Ministry of Education and Xinjiang Uyghur Autonomous Region, Xinjiang University, Urumqi 830046, China
[b] Xinjiang Technical Institute of Physics & Chemistry, CAS, Urumqi 830046, China

ARTICLE INFO

Article history:
Received 28 March 2013
Accepted 11 June 2013
Available online 18 June 2013

Keywords:
Nanocomposites
Microstructure
Optical materials and properties

ABSTRACT

Copper bismuth complex oxides with various novel morphologies were successfully prepared via a hydrothermal process at 120 °C for 3 to 24 h. The structure, morphology, composition and light absorption properties were characterized with XRD, SEM, TEM, HRTEM, EDX and UV–vis diffuse reflectance. The photocatalytic properties under visible light irradiation were evaluated using a degradation experiment. The results showed that some prepared samples exhibited a novel leaf-like nanosheet morphology with a uniform spinel $CuBi_2O_4$ structure, and their excellent visible light absorption characteristics, the photocatalytic properties exhibited a strong dependence on nanocrystal microstructure, morphology and lattice orientation.

1. Introduction

$CuBi_2O_4$ is a recently developed p-type semiconductor material with a spinel-type structure [1] that has been studied for its magnetic and dielectric properties [2], optical properties [3,4] and electrical properties [5]. Generally, Bi(III)-containing compounds have been reported as promising photocatalysts under visible and UV illumination, including $BiVO_4$ [6], $NaBiO_3$ [7], Bi_2WO_6 [8], Bi_2MoO_6 [9] and Bi_3O_4Cl [10]. However, pure $CuBi_2O_4$, having excellent visible light absorption properties [4], is still considered to be lacking in discernible photocatalytic activity due to its high photostability, significant pristine surface and lack of chemical affinity for substrate ions. However, in recent years, the catalytic ability of $CuBi_2O_4$ has been reported for use in the degradation of various types of organic pollutants in the presence of H_2O_2 [11,12] and is expected to develop a new visible light-responsive photocatalysts with high activity through modification, doping and combination [13–15]. Therefore, in the present paper, $CuBi_2O_4$ with various morphologies were synthesized and their visible light-responsive photocatalytic ability was elucidated from the viewpoint of morphology and microstructure.

2. Experimental

Sample preparation: Initially, $Bi(NO_3)_3 \cdot 5H_2O$ was dissolved in deionized water containing concentrated nitric acid. Next, a portion of aqueous $Cu(NO_3)_3 \cdot 3H_2O$ solution was added under constant magnetic stirring followed by the desired amount of NaOH solution added as a precipitation agent. Then, the mixture was diluted to 70 mL and transferred into a Teflon-lined autoclave with an internal volume of 100 mL, maintained at 120 °C for 6 to 24 h. After reaction, the precipitate was collected with a centrifuge, rinsed and then dried overnight at 60 °C in a vacuum oven.

Characterization: The crystal structure was examined by powder XRD (M18XCE, Cu Kα radiation, $\lambda = 1.54056$ Å). The morphology and composition were observed by SEM and EDX (LEO-1430VP), TEM and HRTEM (Hitachi HF-2000). BET measurement (JW-BK) was performed to determine the specific surface areas. UV–vis diffuse reflectance spectra were recorded using a UV–vis double beam spectrophotometer (4802SH) in the wavelength range of 200–1000 nm.

Photocatalytic activity: Photocatalytic evaluation was performed in a reactor containing 100 mL of 0.02 mM methylene blue (MB) dye solution and a designated amount of catalyst in the presence of H_2O_2 at ambient temperature in air under a 500-W xenon lamp. Before irradiation, the solution was stirred for approximately 30 min in the dark followed by H_2O_2 being added, and at the same time, the solution was exposed to light irradiation under magnetic stirring. Next, a 5.0 mL suspension was withdrawn and centrifuged to separate the catalyst at 10 min intervals. The concentration of methylene blue was analyzed by measuring the UV–vis absorption at the maximum absorption wavelength of methylene blue (664 nm).

3. Results and discussion

Crystal structures and morphology: Fig. 1 illustrates the XRD patterns and SEM images of the samples prepared at 120 °C for 6 h (labeled as sample A), 12 h (labeled as sample B, D, E, F) and 24 h

* Corresponding author at: Key Laboratory of Oil and Gas Fine Chemicals, Ministry of Education and Xinjiang Uyghur Autonomous Region, Xinjiang University, Urumqi 830046, China. Tel./fax: +86 991 858 1018.
E-mail address: xyh0707@sina.com (Y. Xie).

0167-577X/$ - see front matter © 2013 Elsevier B.V. All rights reserved.
http://dx.doi.org/10.1016/j.matlet.2013.06.029

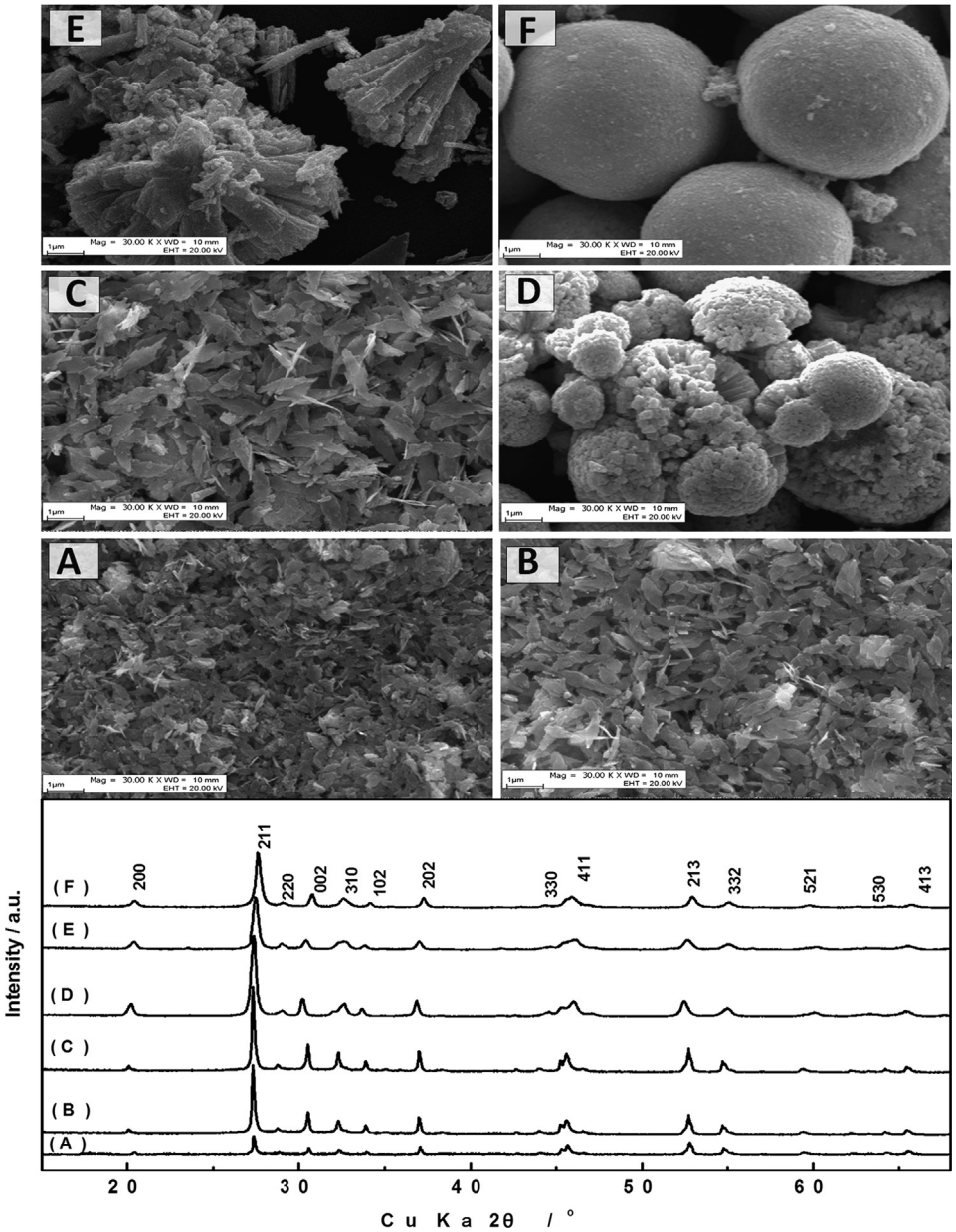

Fig. 1. XRD patterns and SEM images of the samples prepared at 120 °C for 6 (A), 12 (B, D, E, F) and 24 h (C) with the $Cu(NO_3)_2$-to-NaOH molar ratios of 1:30 (A, B, C, D) and 1:10 (E, F) and Cu^{2+} concentrations of 0.02 M (A, B, C, E) and 0.2 M (D, F).

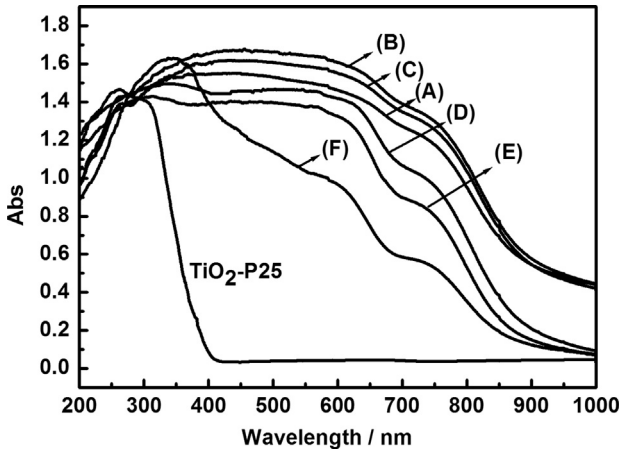

Fig. 2. UV–vis diffuse reflectance spectra of the prepared samples prepared at 120 °C for 6 (A), 12 (B, D, E, F) and 24 h (C) with the $Cu(NO_3)_2$-to-NaOH molar ratios of 1:30 (A, B, C, D) and 1:10 (E, F) and Cu^{2+} concentrations of 0.02 M (A, B, C, E) and 0.2 M (D, F).

(labeled as sample C) with $Cu(NO_3)_2$ to NaOH molar ratios of 1:30 (A, B, C, D) and 1:10 (E, F) and Cu^{2+} concentrations of 0.02 M (A, B, C, E) and 0.2 M (D, F). From Fig. 1, it can be seen that all reflection peaks can be indexed as tetragonal $CuBi_2O_4$ with a spinel-type structure and no impurities (JCPDS file no. 84-1969; $a=8.506$ Å, $c=8.822$ Å). The intensities of the peaks increased following an increase in the treatment time from 6 h to 24 h and the Cu^{2+} concentration had an insignificant influence on the crystallinity and the lattice orientation. The SEM images of (A, B, C) reveal a similar leaf-like, two-dimensional nanosheet morphology with different average crystal sizes of approximately 400, 700, 800 nm in length and 200, 400, 500 nm in width for the samples prepared at 6, 12, and 24 h, respectively. Samples (D) and (E) show distinct morphologies of agglomerated nanorods as a result of the self-assembly method, and sample (F) exhibits perfect microspheres with a mean diameter of 5 μm. From those results, it can be seen that the increased NaOH concentrations and lower Cu^{2+} concentrations were beneficial to the formation of the leaf-like, two-dimensional nanosheets with a good dispersibility. The

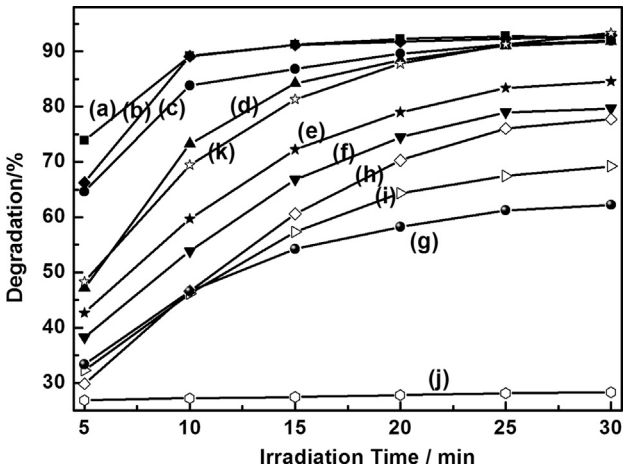

Fig. 3. Effects of $CuBi_2O_4$ on the photocatalytic oxidation of MB under 500-W xenon lamp irradiation. (5.0 (a), 2.0 (b), 0.5 (c) and 0.1 mL (d) H_2O_2)+sample B; 0.1 mL H_2O_2+(sample D (e); sample E (f); sample F (g)); 0.1 mL H_2O_2 (h); TiO_2-P25 (i); pure sample B (j) and 0.1 mL H_2O_2+TiO_2-P25 (k).

specific surface areas of samples B, D, E and F were determined using BET measurement as 35.2, 5.3, 4.9 and 3.1 $m^2\ g^{-1}$ respectively.

UV–vis diffuse reflectance spectroscopy: The UV–vis diffuse reflectance spectroscopy of the prepared $CuBi_2O_4$ samples and the commercial TiO_2-P25 are shown in Fig. 2. It is clear that the optical properties of the $CuBi_2O_4$ samples largely depend on the microstructures and morphologies. In comparison with TiO_2-P25 (Degussa), the prepared samples were found to exhibit significantly enhanced visible light absorption properties, and the samples prepared with the $Cu(NO_3)_2$-to-NaOH molar ratio of 1:30 were found to have the stronger absorption within the visible region. So it can be concluded that the leaf-like, two-dimensional nanosheets were beneficial to the absorption of visible light. According to the UV–vis spectra, the corresponding band gaps of samples B, D, E and F were estimated to be 1.30, 1.34, 1.32 and 1.43 eV respectively.

Photocatalytic degradation: Fig. 3 shows the variation in MB dye concentration with respect to irradiation times for different concentrations of H_2O_2 under 500-W xenon lamp irradiation. From Fig. 3(a, b, c and d), it can be seen that the degradation rate of MB

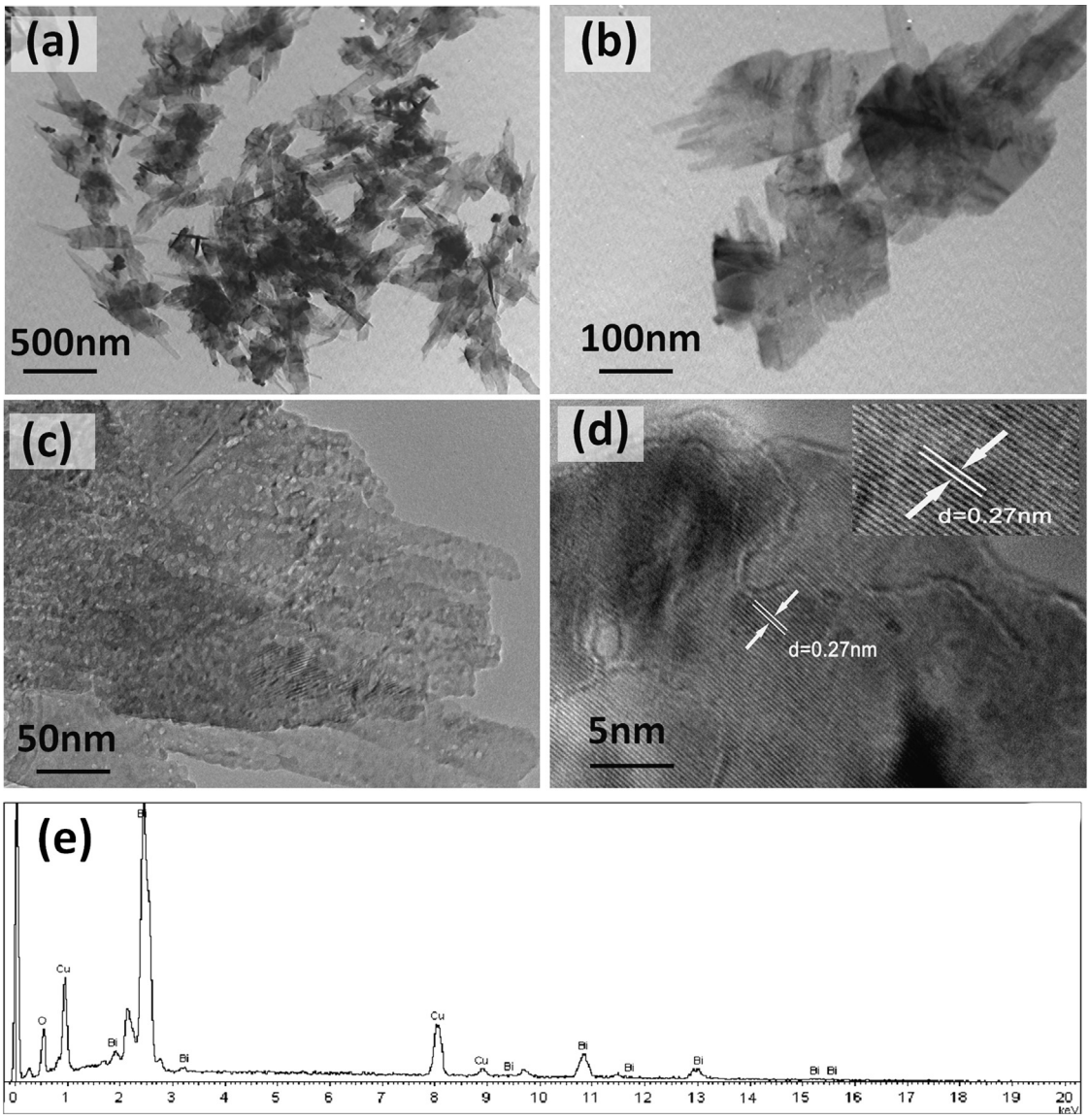

Fig. 4. TEM (a, b), HRTEM (c, d) and EDX (e) results of sample B.

in the presence of 0.08 g sample B increased with increasing amounts of H_2O_2 (from 0.1, 0.5, 2.0 to 5.0 mL), reaching approximately 93% for the reaction time of 20 min. Hence, it can be concluded that the amount of H_2O_2 is not a significant factor with respect to the ultimate degradation rate but that it does reduce the reaction time. Fig. 3(d, e, f and g) shows the effect of the degradation rate on the morphology in the presence of 0.1 mL H_2O_2, and Fig. 3(h) shows the results for only the MB solution with an addition of 0.1 mL pure H_2O_2. It can be clearly seen that the samples with leaf-like, two-dimensional nanosheet structures showed significantly better photocatalytic degradation properties than the agglomerated nanorods and pure H_2O_2, and the morphology was found to strongly affect the photocatalytic efficiency. In contrast, photocatalytic degradation of the MB with only TiO_2-P25 was also performed (Fig. 3(i)) with the result significantly poorer than that of our prepared samples with H_2O_2, but the result of (0.1 mL H_2O_2+TiO_2-P25 (k)) is comparable to that of (0.1 mL H_2O_2+sample B). It is important to note that, when $CuBi_2O_4$ was mixed with H_2O_2, complete degradation of MB occurred under visible light in less than 30 min; however, no obvious degradation was obtained (j) in the case of $CuBi_2O_4$ without H_2O_2 even under light irradiation. Based on these facts, $CuBi_2O_4$ can only be regarded as an assisted-photocatalyst under visible light while in the presence of H_2O_2 but not as a real photocatalyst.

Furthermore, the TEM, HRTEM and EDX are used to illustrate the effect of the assisted-photocatalytic properties on morphology. Fig. 4(a and b) shows the two different magnifications of TEM images of $CuBi_2O_4$ leaf-like nanosheets, which is consistent with their results of SEM. Its detailed HRTEM images are shown in Fig. 4c and d. The distance between the adjacent fringes is about 0.27 nm, which could be indexed to the {310} planes of the tetragonal $CuBi_2O_4$. There is a strong evidence that $CuBi_2O_4$ nanosheets expose the well-defined {310} planes, which is a benefit for better assisted-photocatalytic degradation. The EDS spectra shown in Fig. 4(e) also confirms the formation of $CuBi_2O_4$ and no other impurity is seen.

4. Conclusions

In summary, a facile, low-temperature hydrothermal synthetic route was developed for the preparation of $CuBi_2O_4$ samples with various morphologies. The $Cu(NO_3)_2$-to-NaOH molar ratio and the Cu^{2+} concentration were demonstrated to have significant influences on the morphologies, the methylene blue (MB) dye can be efficiently degraded in the presence of photocatalysts ($CuBi_2O_4$+H_2O_2) under visible light irradiation and that the photocatalytic efficiency is significantly affected by nanocrystal morphology and lattice orientation.

Acknowledgments

This research was financially supported by National Natural Science Foundation of China (21201145); Scientific Research Programmes of Colleges in Xinjiang (XJEDU2010S02) and Open Subject of Key Laboratory of Oil and Gas Fine Chemicals, Ministry of Education and Xinjiang Uyghur Autonomous Region, Xinjiang University (XJDX0908-2011-07).

References

[1] Changkang C, Yongle H, Wanklyn BM, Hodby JW, Wondre FR. J Mater Sci 1993;28(18):5045–9.
[2] Yoshii K, Fukuda T, Akahama H, Kano J, Kambe T, Ikeda N. Physica C 2011;471:766–9.
[3] Abdulkarem AM, Li J, Aref AA, Ren L, Elssfah EM, Wang H, et al. Mater Res Bull 2011;46:1443–50.
[4] Hahn NT, Holmberg VC, Korgel BA, Mullins CB. J Phys Chem C 2012;116:6459–66.
[5] Lyskova NV, Metlinb YG, Belousova VV. Solid State Ionics 2004;166:207–12.
[6] Zhang L, Chen DR, Jiao XL. J Phys Chem B 2006;110(6):2668–73.
[7] Kako T, Zou ZG, Katagiri K, Ye JH. Chem Mater 2007;19:198–202.
[8] Gui MS, Zhang WD, Chang YQ, Yu YX. Chem Eng J 2012;197:283–8.
[9] Shimodaira Y, Kato H, Kobayashi H, Kudo A. J Phys Chem B 2006;110:17790–7.
[10] Chakraborty AK, Kebede MA. React Kinet Mech Catal 2012;106:83–98.
[11] Chen XY, Ma C, Li XX, Chen P, Fang JG. Catal Commun 2009;10:1020–4.
[12] Anandan S, Lee G, Yang C, Ashokkumar M, Wu JJ. Chem Eng J 2012;183:46–52.
[13] Arai T, Yanagida M, Konishi Y, Iwasaki Y. J Phys Chem C 2007;111:7574–7.
[14] Wei L, Shifu C, Sujuan Z, Wei Z, Huaye Z, Xiaoling Y. J Nanopart Res 2010;12:1355–66.
[15] Abdelkader E, Nadjia L, Ahmed B. Appl Surf Sci 2012;258:5010–24.